



# Tauroursodeoxycholic Acid Inhibits *Clostridioides difficile* Toxin-Induced Apoptosis

Colleen M. Pike,<sup>a</sup> John Tam,<sup>b</sup>  Roman A. Melnyk,<sup>b,c,d</sup>  Casey M. Theriot<sup>a</sup>

<sup>a</sup>Department of Population Health and Pathobiology, College of Veterinary Medicine, North Carolina State University, Raleigh, North Carolina, USA

<sup>b</sup>Molecular Medicine, Research Institute, The Hospital for Sick Children, Toronto, Ontario, Canada

<sup>c</sup>Department of Biochemistry, University of Toronto, Toronto, Ontario, Canada

<sup>d</sup>SickKids Proteomics Analytics Robotics Chemical Biology Drug Discovery Facility, Research Institute, Hospital for Sick Children, Toronto, Ontario, Canada

**ABSTRACT** *C. difficile* infection (CDI) is a highly inflammatory disease mediated by the production of two large toxins that weaken the intestinal epithelium and cause extensive colonic tissue damage. Antibiotic alternative therapies for CDI are urgently needed as current antibiotic regimens prolong the perturbation of the microbiota and lead to high disease recurrence rates. Inflammation is more closely correlated with CDI severity than bacterial burden, thus therapies that target the host response represent a promising yet unexplored strategy for treating CDI. Intestinal bile acids are key regulators of gut physiology that exert cytoprotective roles in cellular stress, inflammation, and barrier integrity, yet the dynamics between bile acids and host cellular processes during CDI have not been investigated. Here we show that several bile acids are protective against apoptosis caused by *C. difficile* toxins in Caco-2 cells and that protection is dependent on conjugation of bile acids. Out of 20 tested bile acids, taurine conjugated ursodeoxycholic acid (TUDCA) was the most potent inhibitor, yet unconjugated UDCA did not alter toxin-induced apoptosis. TUDCA treatment decreased expression of genes in lysosome associated and cytokine signaling pathways. TUDCA did not affect *C. difficile* growth or toxin activity *in vitro* whereas UDCA significantly reduced toxin activity in a Vero cell cytotoxicity assay and decreased *tcdA* gene expression. These results demonstrate that bile acid conjugation can have profound effects on *C. difficile* as well as the host and that conjugated and unconjugated bile acids may exert different therapeutic mechanisms against CDI.

**KEYWORDS** *Clostridioides difficile*, apoptosis, bile acids, tauroursodeoxycholic acid, toxin, ursodeoxycholic acid

*Clostridioides difficile* infection (CDI) is a significant public health problem associated with increasing morbidity, mortality, and health care related costs around the globe (1). CDI is a highly inflammatory disease mediated by the production of two large toxins, TcdA and TcdB, that glucosylate and inactivate Rho and Rac GTPases in colonic epithelial cells. Inactivation of these small GTPases disrupts the actin cytoskeleton, ultimately causing apoptosis and a severe inflammatory response (2, 3). Although antibiotics are the first line of treatment, they are the main risk factor in the development of CDI and 10–25% of successfully treated cases experience recurrent infection (4–8). Recent data has indicated an overly robust immune response is more closely correlated with CDI severity than bacterial burden (9–11), thus rather than modulating antibiotic regimens, therapies that target the host response may be a more effective approach.

Bile acids are key regulators of gastrointestinal physiology and drastically influence the *C. difficile* life cycle. Primary bile acids, cholic acid (CA) and chenodeoxycholic acid (CDCA), are synthesized from cholesterol in the liver and are conjugated with either

**Editor** Nancy E. Freitag, University of Illinois at Chicago

**Copyright** © 2022 Pike et al. This is an open-access article distributed under the terms of the [Creative Commons Attribution 4.0 International license](https://creativecommons.org/licenses/by/4.0/).

Address correspondence to Casey M. Theriot, [cmtherio@ncsu.edu](mailto:cmtherio@ncsu.edu).

The authors declare a conflict of interest. C.M.T. consults for Vedanta Biosciences, Inc. and Summit Therapeutics. C.M.T. is a founder of CRISPR Biotechnologies.

**Received** 11 April 2022

**Returned for modification** 17 May 2022

**Accepted** 19 June 2022

**Published** 7 July 2022

taurine or glycine. This conjugation step decreases the hydrophobicity of these molecules, facilitating emulsification and absorption of lipids and nutrients from the small intestine into the portal vein (12, 13). Bile acids that are not reabsorbed by the small intestine are further metabolized by members of the gut microbiota. Several microbes deconjugate, dehydroxylate and epimerize primary bile acids into secondary bile acids (deoxycholic acid (DCA), lithocholic acid (LCA) and ursodeoxycholic acid (UDCA)) that are either excreted or reabsorbed and circulated back to the liver where they are reconstituted with taurine or glycine (14, 15). Members of the microbiota can reconstitute bile acids with several other amino acids such as leucine, phenylalanine and tyrosine which further increases the diversity and complexity of the intestinal bile acid pool (16).

Disruption of bile acid metabolism via diet or antibiotics can have detrimental consequences on gut physiology, including increased susceptibility to gastrointestinal and infectious diseases such as CDI (17–19). Prior to antibiotic treatment, microbial-derived secondary bile acids inhibit *C. difficile* growth (18, 20). Protection conferred by secondary bile acids is lost after antibiotics whereas primary bile acids levels increase, supporting *C. difficile* spore germination and outgrowth (21). Aside from directly inhibiting bacterial growth, bile acids can elicit protection against CDI through additional mechanisms. Several bile acids neutralize TcdB's cytotoxicity by directly binding to the CROP domain, blocking TcdB-receptor binding and preventing entry into host cells (22). Oral administration of bile acids can alter host inflammation. Mice given UDCA prior to *C. difficile* challenge had less colonic edema associated with altered expression of genes in the NF- $\kappa$ B pathway (23). This was the first indication that bile acids may alter the host response during CDI, however it unclear whether this is due to activity against *C. difficile*, the host or both.

Bile acids are potent modulators of intestinal membrane integrity and cell signaling pathways (24), yet little attention has been given to how these metabolites influence the host during CDI. Several bile acids with anti-inflammatory properties are in clinical trials for inflammatory diseases such as inflammatory bowel disease and CDI (25, 26). Mechanistically, bile acids can maintain intestinal barrier integrity, attenuate apoptosis, cytokine production and improve cell survival (25, 27). We therefore hypothesized that the cytoprotective properties of bile acids can be leveraged against damage caused by *C. difficile* toxins. Here, we screened 20 host- and microbiota-derived bile acids for their ability to inhibit toxin-induced apoptosis in Caco-2 cells. We found that several conjugated bile acids significantly inhibited toxin-induced caspase-3/7 activation with tauroursodeoxycholic acid (TUDCA) being the most potent inhibitor. TUDCA altered the Caco-2 transcriptional profile, decreasing the expression of genes involved in lysosome function and cytokine signaling. The unconjugated form of TUDCA, UDCA, did not attenuate caspase-3/7 activation but significantly decreased *C. difficile* toxin activity and gene expression of *tcdA* *in vitro*. Conversely, TUDCA had no effect on *C. difficile* pathogenesis *in vitro*. Collectively, our results demonstrate that cytoprotective bile acids elicit can be leveraged against *C. difficile* toxins and that bile acid conjugation can have profound effects on both *C. difficile* and the host.

## RESULTS

**Conjugated bile acids inhibit toxin-induced caspase activation.** Apoptosis induced by *C. difficile* toxins causes extensive colonic tissue damage, initiating inflammatory cascades that manifest as the detrimental symptoms of CDI (2, 28). Given that several bile acids have potent anti-apoptotic activity (25), we probed whether bile acids can inhibit toxin-induced apoptosis in human intestinal Caco-2 cells (29). Monolayers of Caco-2 cells were treated with recombinantly purified TcdA and TcdB (30 pM) for 8 h before the addition of 20 individual conjugated and unconjugated bile acids. Bile acids and toxins were added asynchronously to avoid effects that could be a result of direct binding between them (22). The colon contains a higher concentration of unconjugated bile acids (~200  $\mu$ M to 1 mM) due to conjugated bile acids being either reabsorbed in

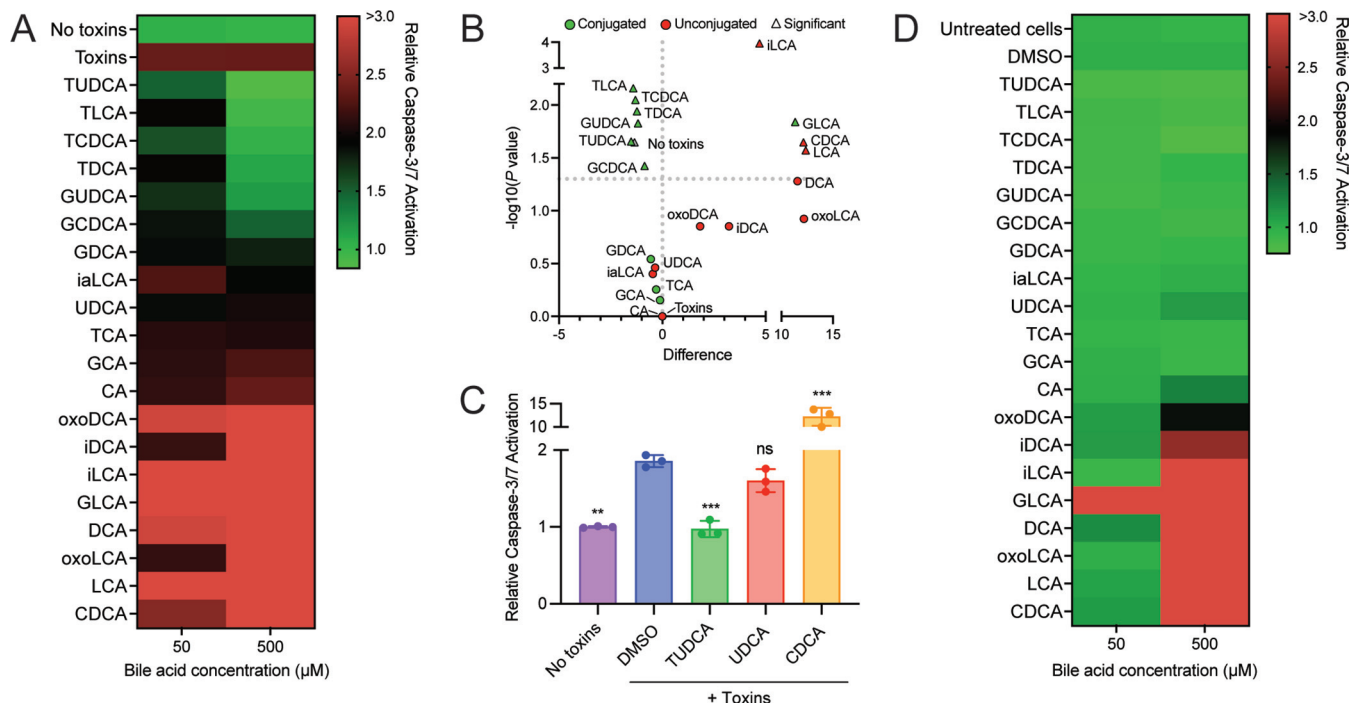


**FIG 1** Conjugated bile acids inhibit toxin-induced caspase-3/7 activation in Caco-2. (A) Relative caspase-3/7 activation in Caco-2 cells 24 h after treatment with recombinantly purified TcdA and TcdB (30 pmol) and the listed bile acids. Cells were pre-incubated with toxins for 8 h before the addition of bile acids. Data are represented as the ratio of caspase activation RFU to cell viability RFU and relative to no toxins. The colors on the heatmap represent low (green) to high (red) relative caspase activation. (B) The mean difference in relative caspase-3/7 activation between intoxicated cells treated with and without bile acids (500 μM) plotted against  $-\log_{10}(P \text{ value})$ . Green data points indicate conjugated bile acids and red data points indicate unconjugated bile acids. No toxins and toxins data points are in gray. Triangle shaped data points are significant ( $p < 0.05$ ; Student's *t* test). (C) Relative caspase-3/7 activation in HCT116 cells pretreated with recombinantly purified TcdA and TcdB (30 pmol) for 8 h and the listed bile acids (500 μM) after 48 h. (D) Relative caspase-3/7 activation in Caco-2 cells 24 h after treatment with the listed bile acids with no toxins. Student's *t* test; \*,  $P < 0.05$ ; \*\*,  $P < 0.01$ ; \*\*\*,  $P < 0.001$ . Abbreviations: TUDCA, tauroursodeoxycholic acid; TLCA, tauroolithocholic acid; TCDCa, taurochenodeoxycholic acid; TDCA, taurodeoxycholic acid; GUDCA, glyoursodeoxycholic acid; GCDCA, glyochenodeoxycholic acid; GDCA, glycodeoxycholic acid, iaLCA, iso-allo-lithocholic acid; UDCA, ursodeoxycholic acid; TCA, taurocholic acid; GCA, glycocholic acid; CA, cholic acid; oxoDCA, 3-oxo-deoxycholic acid; iDCA, iso-deoxycholic acid; iLCA, iso-lithocholic acid; oxoLCA, 3-oxo-lithocholic acid; GLCA, glycolithocholic acid; DCA, deoxycholic acid; LCA, lithocholic acid; CDCA, chenodeoxycholic acid.

the small intestine or deconjugated by the microbiota. We treated Caco-2 cells with two concentrations well below critical micelle concentrations, 50 μM and 500 μM, to observe concentration-dependent effects.

Caspase-3/7 activation and cell viability were measured 24 h after the addition of bile acids (Fig. 1A and Fig. S1 in the supplemental material). Data are displayed as the ratio of caspase-3/7 activation relative fluorescence units (RFU) to cell viability RFU and relative to the no toxin control. A Student's *t* test was used to identify bile acids that significantly decreased caspase-3/7 activation relative to cells treated with toxins. After plotting the mean difference in relative caspase-3/7 activation against  $-\log_{10}(P \text{ value})$ , we observed a trend between caspase activation and bile acid conjugation (Fig. 1B); only conjugated bile acids decreased toxin induced caspase-3/7 activation whereas glycolithocholic acid (GLCA) and several unconjugated bile acids exacerbated caspase-3/7 activation. TUDCA was the only bile acid treatment to significantly reduce caspase-3/7 activation at 50 μM ( $P = 0.042$ ). At 500 μM, TUDCA, taurodeoxycholic acid (TDCA), tauroolithocholic acid (TLCA), taurochenodeoxycholic acid (TCDCa), glyoursodeoxycholic acid (GUDCA), and glyochenodeoxycholic acid (GCDCA) significantly decreased caspase-3/7 activation (TUDCA  $P = 0.02$ , TDCA  $P = 0.0011$ , TLCA  $P = 0.006$ , TCDCa  $P = 0.0008$ , GUDCA  $P = 0.014$ , GCDCA  $P = 0.004$ ). Conversely, at 50 μM, GLCA, LCA, and DCA augmented caspase-3/7 activation but only GLCA was significant (GLCA  $P = 0.03$ , LCA  $P = 0.12$ , DCA  $P = 0.17$ ). GLCA also significantly induced caspase-3/7 activation in the absence of toxins ( $P < 0.001$ ; Fig. 1D), indicating GLCA is toxic to Caco-2 cells on its own. At 500 μM, one conjugated (GLCA), four unconjugated (DCA, GLCA, LCA, CDCA) and four bile acid derivatives (oxoLCA, oxoDCA, iLCA and iDCA) increased

caspase-3/7 activation, with iLCA, LCA, CDCA and GLCA causing a significant increase (iLCA  $P < 0.0001$ , LCA  $P = 0.02$ , CDCA  $P = 0.02$ , GLCA  $P = 0.014$ ). Similar to the findings of previous reports (30), several unconjugated bile acids (CDCA, DCA, LCA, GLCA, oxoDCA, isoDCA, isoLCA, and oxoLCA) induced apoptosis on their own in the absence of toxins (Fig. 1D). Conjugated bile acids, with the exception of GLCA, did not alter apoptosis in the absence of toxins at either concentration.

To validate these results, we repeated this assay using another human colorectal carcinoma cell line, HCT116. Using the same experimental set up as described previously, caspase-3/7 activation was measured in intoxicated HCT116 cells treated with TUDCA, UDCA, or CDCA (500  $\mu\text{M}$ ). Similar to our findings in Caco-2 cells, TUDCA decreased, CDCA exacerbated, and UDCA did not change toxin-induced caspase-3/7 activation (no toxins  $P = 0.002$ , TUDCA  $P < 0.001$ , CDCA  $P = 0.01$ , UDCA  $P = 0.07$ ; Student's  $t$  test; Fig. 1C). These findings suggest that several bile acids can inhibit toxin induced caspase-3/7 activation and that bile acid conjugation can influence the host response to toxins.

**TUDCA and not UDCA exhibit potent anti-apoptotic activity against *C. difficile* toxins.** Of the 20 bile acids tested in our screen, TUDCA was the most inhibitory against toxin-induced apoptosis. Both TUDCA and UDCA have been established as potent inhibitors of apoptosis but their cytoprotective properties have not been leveraged against *C. difficile* toxins (25). We therefore further characterized the inhibitory effects of TUDCA and UDCA against toxins.

Several bile acids directly bind to TcdB, blocking TcdB from binding host cell receptors and being endocytosed (22), however it is unknown whether TUDCA or UDCA can bind to TcdB. We assessed the direct binding between bile acids and recombinantly purified TcdB using differential scanning fluorimetry in which direct binding between bile acids and TcdB will result in an increased melting temperature of TcdB (Fig. 2A). The estimated  $\text{EC}_{50}$  (half maximal effective concentration) of TUDCA and UDCA binding was 338  $\mu\text{M}$  and  $>1000 \mu\text{M}$ , respectively. Positive control TCDCA bound with an  $\text{EC}_{50}$  of 77  $\mu\text{M}$ , while the  $\text{EC}_{50}$  of negative control dehydrocholate was  $>1,000\mu\text{M}$ . To determine if binding between bile acids and TcdB inhibits TcdB-receptor binding and downstream cytotoxicity, we tested the ability of UDCA and TUDCA to inhibit TcdB-induced cell rounding in IMR90 cells by measuring cell rounding index (Fig. 2B and C). In this assay, direct binding between bile acid and TcdB will result in a reduction in IMR90 cell rounding. IMR90 cells were concurrently treated with recombinantly purified TcdB and increasing concentrations of TUDCA or UDCA for 3 h before cell rounding was measured. The  $\text{EC}_{50}$  of inhibition by TUDCA and UDCA were  $>800 \mu\text{M}$  and  $>400 \mu\text{M}$ , respectively. Positive and negative control bile acids TCDCA and dehydrocholate had an  $\text{EC}_{50}$  of 75  $\mu\text{M}$  and  $>400 \mu\text{M}$ , respectively. In IMR90 fibroblasts, TcdB induced cell rounding in the presence of TUDCA and UDCA, indicating these bile acids do not interfere with TcdB receptor binding and endocytosis. TUDCA and UDCA did not bind to TcdA or alter TcdA-induced cell rounding (data not shown).

We next evaluated the effects of a fixed dose of TUDCA and UDCA (500  $\mu\text{M}$ ) against increasing concentrations of TcdB (Fig. 2D). TUDCA significantly reduced caspase-3/7 activation in cells treated with all tested TcdB concentrations (0.01 pM,  $P = 0.0001$ ; 0.1 pM,  $P = 0.001$ ; 1 pM,  $P < 0.0001$ ; 10 pM,  $P < 0.0001$ ; 100 pM,  $P < 0.0001$ ; two-way ANOVA). UDCA was only inhibitory against 1 pM concentration of TcdB ( $P < 0.0001$ ). This suggests that UDCA is less potent than its taurine conjugated form. In addition to using recombinant purified toxins to induce apoptosis, we tested the anti-apoptotic activity of TUDCA and UDCA against endogenously produced toxins. Caco-2 cells were treated with filtered supernatants from either a wild-type (*C. difficile* R20291) or toxin-null strain of *C. difficile* (1:500) for 8 h. DMSO, TUDCA, or UDCA (500  $\mu\text{M}$ ) were added, and caspase activation was measured 24 h later (Fig. 2E). Compared to cells treated with DMSO, TUDCA and not UDCA significantly decreased caspase activation (TUDCA,  $P = 0.001$ ; UDCA,  $P = 0.058$ ; Student's  $t$  test). The supernatant from the toxin-null strain did not induce apoptosis, indicating that TUDCA's inhibitory effect was directly against toxins.

Lastly, we tested whether TUDCA inhibits staurosporine-induced apoptosis in Caco-2

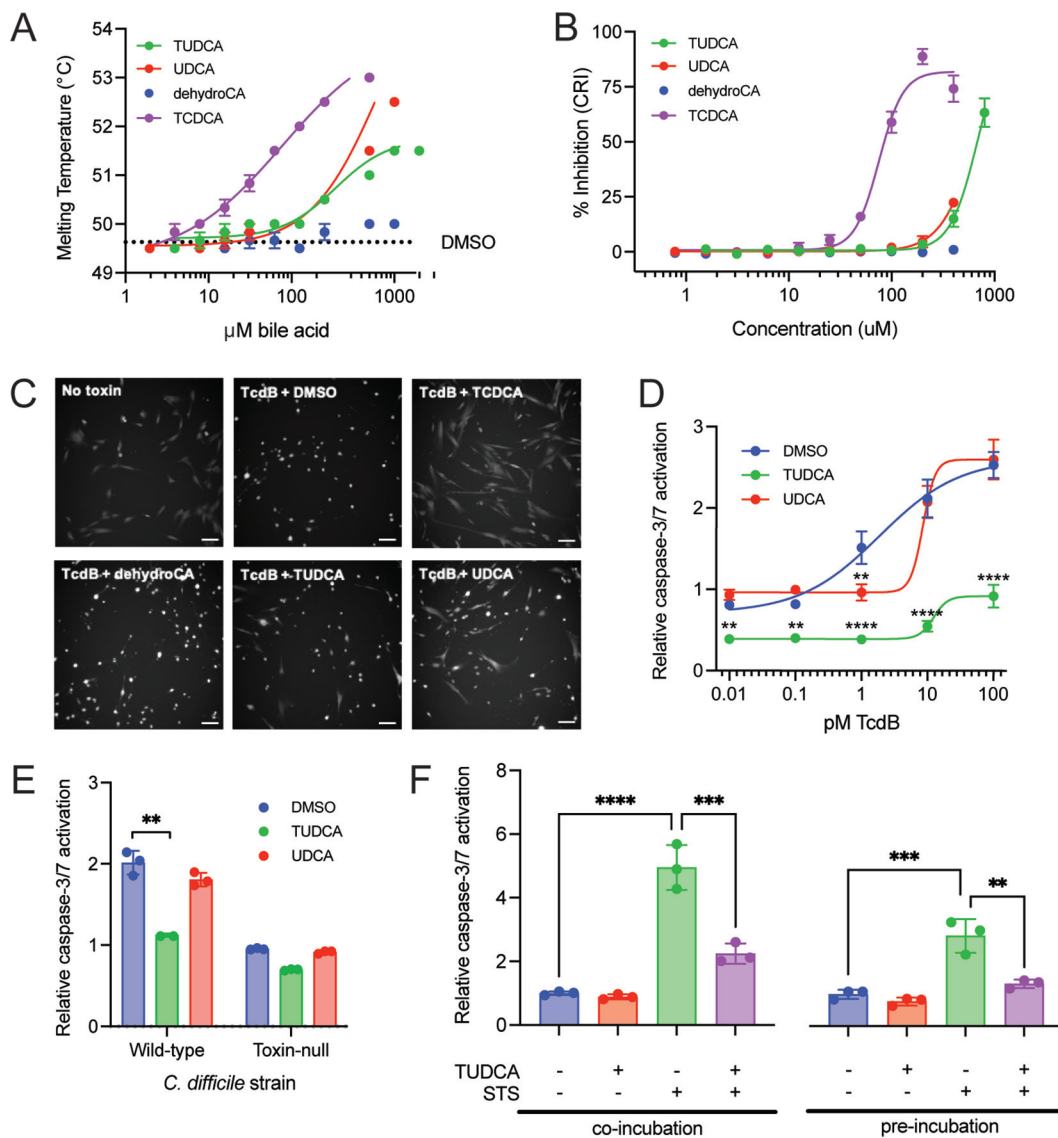


**FIG 2** TUDCA and not UDCA exhibits potent anti-apoptotic activity against *C. difficile* toxins. (A) Titration curves of increasing bile acids by DSF. Bars represent SEM of three separate experiments. (B) Intoxication of IMR90 fibroblasts measured by cell rounding index (CRI). The EC50s of inhibition by TUDCA and UDCA were  $>800\mu\text{M}$  and  $>400\mu\text{M}$ , respectively. Positive and negative control bile acids TCDCa and dehydrocholate had an EC50 of  $75\mu\text{M}$  and  $>400\mu\text{M}$ , respectively. (C) Representative images of IMR90 fibroblasts from CRI assay in from Fig. 2B Cells were treated with DMSO or bile acid along with 0.5pM TcdB, and images were collected 3.5 h later (Scale bars,  $100\mu\text{m}$ ). The concentrations of bile acids were:  $200\mu\text{M}$  TCDCa,  $400\mu\text{M}$  dehydrocholate,  $400\mu\text{M}$  TUDCA,  $400\mu\text{M}$  UDCA. (D) Relative caspase-3/7 activation of Caco-2 cells treated with  $500\mu\text{M}$  the listed bile acids and increasing concentrations of recombinantly purified TcdB. Cells were treated with TcdB for 8 h before the addition of bile acids. (E) Relative caspase-3/7 activation of Caco-2 cells treated with  $500\mu\text{M}$  the listed bile acids and filtered supernatants from wild-type or toxin-null *C. difficile* strains (1:500). Cells were treated with supernatants for 8 h before the addition of bile acids. (F) Relative caspase-3/7 activation of Caco-2 cells either co-incubated with  $1\mu\text{M}$  staurosporine (STS) and  $500\mu\text{M}$  TUDCA or pre-incubated with staurosporine for 8 h before the addition of TUDCA. Bars represent SEM of three separate experiments. (A-D) Student's *t* test with Welch's correction; (E) One-way ANOVA with Sidak's multiple-comparison test. \*\*,  $P < 0.01$ ; \*\*\*,  $P < 0.001$ ; \*\*\*\*,  $P < 0.0001$ .

cells (Fig. 2F). Cells were either co-incubated with TUDCA ( $500\mu\text{M}$ ) and staurosporine ( $1\mu\text{M}$ ) or pretreated with staurosporine for 8 h before the addition of TUDCA. Caspase-3/7 activation was measured 24 h later. Similar to previous findings, TUDCA inhibited staurosporine-induced caspase-3/7 activation in both the co- and pre-incubation experiments ( $P = 0.002$ ,  $P = 0.0012$ , respectively; one-way ANOVA).

**TUDCA alters the transcriptome of toxin-treated Caco-2 cells.** To determine how TUDCA alters the host response to toxins, we compared gene expression profiles of

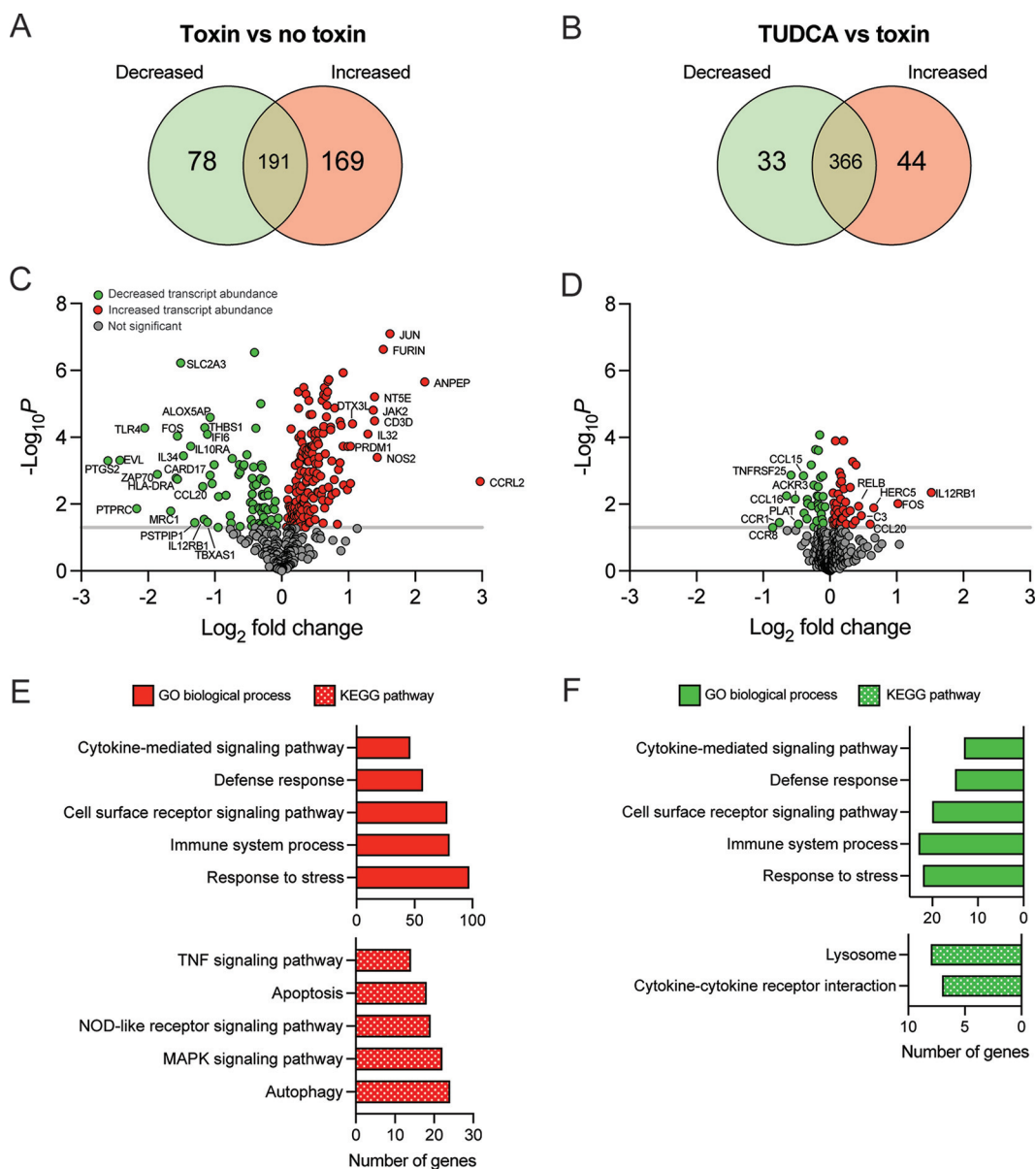


**FIG 3** TUDCA alters the transcriptome of toxin-treated Caco-2 cells. (A, B) Venn diagram depicting the significant differentially expressed genes (DEGs) in intoxicated Caco-2 cells treated with (left) toxins relative to no toxins and (right) TUDCA relative to toxins (increased expression, yellow; decreased expression, purple). (C, D) Volcano plots displaying  $\log_2$  fold change plotted against  $-\log_{10}(P)$  value of DEGs in intoxicated Caco-2 cells treated with (left) toxins relative to no toxins and (right) TUDCA relative to toxins. Red data points highlight genes with increased fold change, green data points highlight genes with decreased fold change, and gray data points highlight genes with insignificant fold changes. (E, F) GO biological terms and KEGG pathways of (left) toxin relative to no toxin DEGs with increased abundance and (right) TUDCA relative to toxin DEGs with decreased abundance (FDR cut off 0.05).

untreated, toxin treated, and TUDCA+toxin treated cells (referred to as no toxins, toxins and TUDCA, respectively). Caco-2 cells were grown in 24-well plates and treated with TcdA and TcdB (30 pmol) for 8 h before TUDCA was added (500  $\mu$ M). RNA was isolated 24 h later and analyzed using the NanoString Host Response panel. We first assessed how toxins altered Caco-2 gene expression relative to no toxins. After processing the raw data using nSolver, 438 transcripts were above threshold level (probe count > 20); 247 genes had a significant fold change in expression with 169 transcripts being increased and 78 transcripts being decreased (Fig. 3A and C, Table S3 in the supplemental material). Gene set enrichment analysis identified cytokine-mediated signaling,

defense response, cell surface receptor signaling, immune system process, and response to stress as enriched gene ontology (GO) biological process terms in differentially expressed genes (DEGs) with increased abundance (Fig. 3E, Table S4). Pathway enrichment analysis identified TNF signaling, apoptosis, NOD-like receptor signaling, MAPK signaling and autophagy as enriched KEGG pathways in DEGs with increased abundance (Fig. 3E). This transcriptional profile is in line with previous findings that toxins induce cytotoxic and inflammatory signaling pathways.

We next compared gene expression profiles of Caco-2 cells treated with TUDCA and toxins relative to toxins alone. nSolver detected 476 transcripts above threshold level (probe count > 20); 77 genes had a significant fold change in expression, with increased expression in 33 genes and decreased expression in 44 genes (Fig. 3B and D, Table S5 in the supplemental material). However, the fold change were relatively low with only two genes being above a 1-fold change (*FOS* and *IL12RB1*). The GO biological process terms identified among the DEGs with decreased abundance matched the GO terms associated with toxin treatment (Fig. 3F and Table S6), suggesting TUDCA decreased the expression of several genes involved in cell stress and immune signaling pathways induced by toxins. The lysosome and cytokine-cytokine receptor interaction signaling KEGG pathways were enriched in DEGs with decreased abundance (Fig. 3F).

Decreased expression of several genes involved in lysosome function, including vacuolar ATPases *TCIRG1* and *ATP6V0D1*, led us to speculate that TUDCA may alter the pH of endosomal compartments. Acidification of endocytic vesicles is required for the release of the cytotoxic glucosyltransferase domain from the endosome (31). Several small molecules inhibit endosomal acidification thereby preventing pore formation and translocation of toxins into the cytosol (32). To assess the effect of TUDCA and UDCA on endosomal pH, we quantified lysotracker staining in IMR90 cells treated with increasing concentrations of bile acids (Fig. S2 in the supplemental material). We observed no change in lysotracker staining, indicating that TUDCA does not alter cellular pH and may instead modulate other lysosome associated processes like autophagy.

Several transcripts (*CCR1*, *CCL15*, *CCL16*, and *MYC*) were selected for further qRT-PCR analysis to validate the NanoString results (Fig. S3 in the supplemental material). Relative to toxin-treated cells, TUDCA treatment significantly decreased expression of *CCR1*, *CCL15* and *CCL16* and increased expression of *MYC* (*CCR1*,  $P = 0.046$ ; *CCL15*,  $P = 0.046$ ; *CCL16*,  $P = 0.041$ ; *MYC*,  $P = 0.003$ ; Student's *t* test). These findings were similar to the trends observed in the NanoString data.

Treatment with TUDCA alone did not yield a robust change in the Caco-2 gene expression profile relative to untreated Caco-2 cells. nSolver software identified 27 significant DEGs with a decrease in 23 transcripts and increase in four transcripts (Table S7 in the supplemental material).

**TUDCA and UDCA alter different phases of the *C. difficile* lifestyle *in vitro*.** UDCA alters *C. difficile* spore germination, vegetative cell growth and toxin activity *in vitro*, but TUDCA's influence on these processes *in vitro* has not been investigated (23). To determine the effect of TUDCA on spore germination, *C. difficile* spores were added to BHI containing 1% of the spore germinant, TCA, and either CDCA (0.04%, a potent inhibitor of spore germination), TUDCA or UDCA. Spore germination was measured as the decrease in OD<sub>600</sub> measured every 20 min over 1 h. Cultures grown in TCA had a significant drop in OD<sub>600</sub> after 20 min whereas the OD<sub>600</sub> of cultures grown in CDCA did not change over the 1-h period (Fig. 4A). Similar to CDCA, cultures grown in either UDCA and TUDCA did not drop in OD<sub>600</sub> over 1 h, indicating that both bile acids inhibit TCA-induced spore germination.

We next tested the ability of TUDCA to alter *C. difficile* growth by enumerating CFU/mL after 24 h of anaerobic growth in BHI containing either DMSO, TUDCA or UDCA (500  $\mu$ M; Fig. 4B). Similar to previous findings, UDCA significantly increased *C. difficile* growth ( $p < 0.0001$ ; two-way ANOVA with Sidak's multiple comparison test). TUDCA had no effect on growth ( $p = 0.1436$ ). From the same cultures, we measured toxin activity from *C. difficile* supernatant using a Vero cell rounding assay. Supernatants were

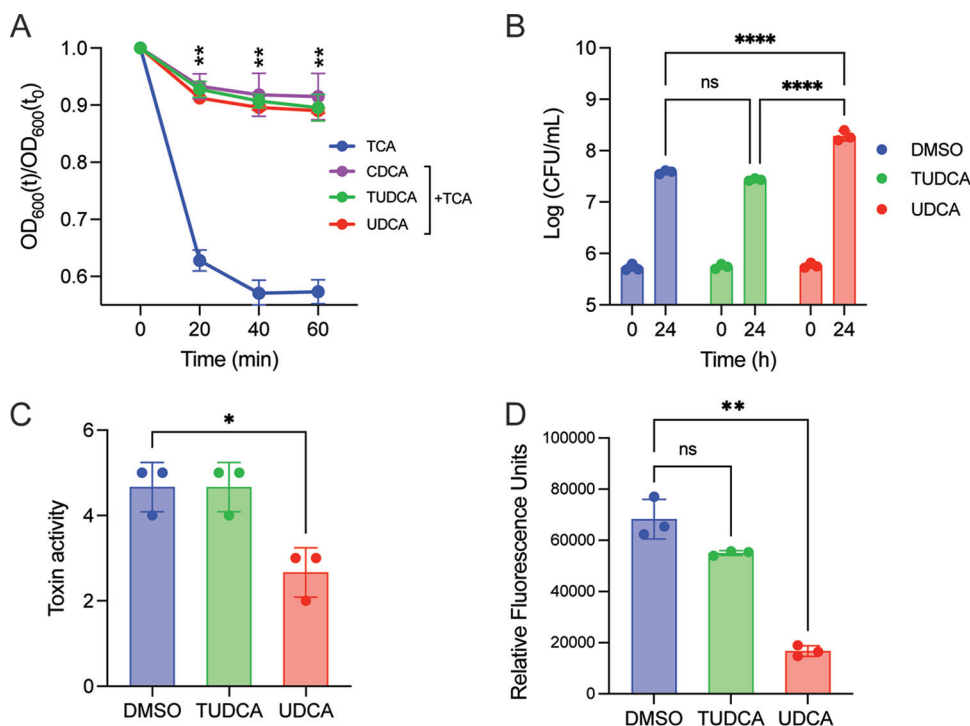


**FIG 4** TUDCA and UDCA alter different phases of the *C. difficile* life cycle *in vitro*. (A) *C. difficile* spores were grown in the presence of the spore germinant, TCA, and 500  $\mu$ M the listed bile acids. Germination was monitored by plotting the ratio of the OD<sub>600</sub> at the listed time points to the OD<sub>600</sub> at time zero. (B) Culture aliquots of *C. difficile* taken at 0 and 24 h were enumerated on BHI plates to obtain CFU/mL of total vegetative cells. (C) Filtered culture supernatants after 24 h of growth were used for a Vero cell cytotoxicity assay. Toxin activity is expressed as log<sub>10</sub> reciprocal dilution toxin per 100  $\mu$ L of *C. difficile* culture supernatant. (D) *C. difficile* carrying a *PtcdA-mCherry* reporter plasmid was grown for 24 h with the listed treatments. Data are displayed as the ratio of fluorescence to absorbance. (B) Two-way ANOVA with Sidak's multiple comparison test, (C and D) Student's *t* test with Welch's correction. All experiments were performed in triplicate. \*, *P* < 0.05; \*\*, *P* < 0.005; \*\*\*\*, *P* < 0.0001. mean and error bars indicate the sd. \*, *P* < 0.05; \*\*, *P* < 0.005; \*\*\*, *P* < 0.0005; Student's *t* test; *n* = 4.

filtered, serially diluted, and added to Vero cells in a 96-well plate. Cell rounding was assessed 24 h later (Fig. 4C). Compared to the DMSO control, UDCA significantly decreased toxin activity while TUDCA had no effect on toxin activity (UDCA *P* = 0.0132, TUDCA, *p* > 0.9999; Student's *t* test).

Our differential scanning fluorimetry (DSF) results revealed that the EC<sub>50</sub> of UDCA and TcdB binding is >1,000  $\mu$ M, thus the decreased toxin activity is not attributed to direct binding and neutralization of TcdB cytotoxicity. To determine how UDCA could be altering toxin activity, we assessed whether UDCA alters toxin expression using a fluorescent reporter plasmid. *C. difficile* carrying the pDSW1728 plasmid encoding the *tcdA* promoter upstream of *mCherry* was grown in BHI + thiamphenicol supplemented with DMSO, TUDCA or UDCA (500  $\mu$ M) and red fluorescence was measured 24 h later. Data are represented as the ratio of fluorescence to OD<sub>600</sub> (Fig. 4D). *C. difficile* carrying the pDSW1728 plasmid with no *PtcdA-mCherry* cassette was used as a negative control and produced no fluorescence after 24 h of growth. We observed a significant reduction in normalized fluorescence in *C. difficile* grown in UDCA compared to the DMSO control (*P* = 0.004, Student's *t* test). No significant reduction in fluorescence was observed in *C. difficile* grown in TUDCA compared to DMSO (*P* = 0.09). These data demonstrate that TUDCA and UDCA exert different effects on the *C. difficile* life cycle *in vitro*.

## DISCUSSION

Inflammation is suggested to benefit *C. difficile*, as patients with inflammatory bowel disease are four times more likely to acquire CDI, and a shift in the nutrient availability in

the inflamed mouse gut may offer an alternative nutrient source for *C. difficile* (33–35). Immune cell infiltration is necessary for mounting an early defense against CDI (36, 37), however a robust inflammatory response can be detrimental, as prolonged exposure to proinflammatory mediators can exacerbate tissue damage (9, 38, 39). Thus, therapies that target inflammation and the host response during CDI could potentially decrease disease severity and disease recurrence. Bile acids act as an important communication system between the intestinal lumen and the liver, influencing bile acid synthesis, barrier maintenance and inflammatory pathways (24). The *C. difficile* life cycle is sensitive to different bile acids, yet the dynamics between bile acids and host cellular responses during CDI have been given little attention. We found that several bile acids alleviated toxin-induced caspase-3/7 activation in Caco-2 cells. Similar to previous findings, caspase inhibition was dependent on bile acid conjugation (30, 40). Several taurine and glycine conjugated bile acids were protective whereas unconjugated bile acids exacerbated toxin-induced apoptosis. CDCA, DCA, and LCA can activate the intrinsic apoptosis pathway at concentrations below their critical micelle concentrations by inducing oxidative stress and altering mitochondria membrane permeability (41). This could explain why several unconjugated bile acids augmented toxin-induced apoptosis.

It is well established that antibiotics disrupt the gut microbiota, depleting secondary bile acids and increasing susceptibility to CDI (18). Given that secondary bile acids regulate multiple host cell processes in the gut (24), the loss of these key cell signaling molecules is expected to also impact the host response, yet this association in the context of CDI has not been explored. We found that conjugated secondary bile acids (TUDCA, GUDCA, TCDCA, GCDCA, GDCA, TLCA) decrease toxin induced caspase-3/7 activation. This class of bile acid is lost after antibiotic use, thus restoring these protective bile acids could be used as a treatment strategy to attenuate cellular damage and inflammation caused by *C. difficile* toxins.

Of our screen of 20 bile acids, TUDCA was the most inhibitory against toxin-induced apoptosis. UDCA was the only unconjugated bile acid to not increase toxin-induced apoptosis, possibly due to its low hydrophobicity. GUDCA treatment also yielded significant protection, signifying that bile acid conjugation can have varying effects on the host response. Previous work from our group has shown that mice pretreated with an oral gavage of UDCA had an attenuated host inflammatory response in a mouse model of CDI (23). Metabolomics of stool from the same study found that mice treated with UDCA had an almost 5-fold increase in TUDCA compared to UDCA. Mice do not produce glycine conjugated bile acids, thus only an increase in taurine conjugation was observed. This elevated concentration of TUDCA is presumably due to the conjugation of taurine to UDCA by conjugative liver enzymes. Due to the extensive increase in TUDCA, it is unclear which bile acid is responsible for altering the host inflammatory response during CDI. Our results suggest that TUDCA may partly contribute to the protection conferred by UDCA administration. Interestingly, both TUDCA and UDCA have been reported to attenuate apoptosis but only TUDCA was inhibitory against toxin induced caspase-3/7 activation (23). UDCA and TUDCA both modulate mitochondria permeabilization and release of pro-apoptotic signals. Mitochondria permeabilization partly contributes to toxin-induced apoptosis, thus it is unclear why UDCA was not protective (42, 43). UDCA decreased toxin activity and *tcdA* gene expression which is in line with *in vivo* findings that UDCA administration significantly inhibited toxin activity in the mouse cecum on day 4 (23). Taken together, our data suggests administration of UDCA may offer a dual method of protection against CDI, with TUDCA modulating the host cell response and UDCA targeting toxin production.

We used NanoString to understand how toxins and TUDCA alter Caco-2 cell gene expression. Relative to untreated cells, toxin treated cells caused significant fold changes in 247 genes. In DEGs with increased abundance, autophagy, apoptosis, TNF signaling and NOD-like receptor signaling KEGG pathways were enriched. The addition of TUDCA to intoxicated Caco-2 cells resulted in significant fold changes in only 77 genes. This relatively low number of DEGs may indicate that TUDCA acts at the protein level rather than

the transcriptional level to inhibit toxin-induced apoptosis. TUDCA has endoplasmic reticulum chaperone activity and can modify Rac1 GTPase *in vitro*, corroborating this hypothesis (44, 45). Of the DEGs with decreased abundance, five genes were in the cytokine-cytokine receptor interaction KEGG pathway (*CCR1*, *CCL15*, *CCL16*, *IL1R2*, *IL17RA*), several of which have been implicated in inflammatory intestinal diseases. *CCL15* and *CCL16* are the ligands of receptor *CCR1*; receptor binding mediates chemotaxis of neutrophils, monocytes and lymphocytes (46). *CCR1*<sup>-/-</sup> mice had less ileal epithelial cell damage and immune cell infiltration in response to TcdA (47). *IL-17RA* is the receptor for the proinflammatory cytokine *IL-17*. The role of *IL-17RA* signaling in inflammation has produced conflicting results, as *IL-17RA*<sup>-/-</sup> mice were protected from trinitrobenzenesulfonic induced colitis, whereas mice given a neutralizing antibody against *IL-17RA* experienced exacerbated inflammation in response to DSS-induced colitis (48, 49). TUDCA is anti-inflammatory against several diseases, but has not been previously shown to alter expression of this set of genes. TUDCA treatment also decreased expression of eight lysosome-associated genes, including *LAMP1*. While TUDCA's direct role in lysosome function has not been explored, TUDCA has been shown to modulate autophagy. Fusion between lysosomes and autophagosomes is a key step in the progression of autophagy. Two studies reported that TUDCA decreased autophagy and protein levels of *LAMP1* in both TGF- $\beta$ 1 treated fibroblasts and in a mouse model of Parkinson's Disease (50, 51). TUDCA may attenuate autophagy caused by *C. difficile* toxins, although further proteomic and phenotypic analyses are needed to pinpoint the direct mechanism between TUDCA and these pathways.

While this study is limited in that bile acid mediated protection was only studied in Caco-2 cells, several pieces of evidence suggest that TUDCA has therapeutic applications against inflammatory diseases in both mouse models and humans. UDCA is currently in a phase 4 clinical trial for recurrent CDI and TUDCA is in a phase 1 trial for ulcerative colitis. Several studies have shown that in dextran sodium sulfate-induced mouse models of colitis, TUDCA decreases inflammation and improves survival rates (52–55). Mechanistically, these same studies found that TUDCA decreased apoptosis, the unfolded protein response and production of inflammatory markers. TUDCA is known to inhibit apoptosis caused by different pro-apoptotic stimuli including staurosporine, TNF, LPS and FasL (53). Supporting previous findings, we found that TUDCA inhibits staurosporine-induced apoptosis in Caco-2 cells in both co- and pre-incubation conditions. We propose that the protection conferred by TUDCA observed in this work is most likely not specific to *C. difficile* toxins, but rather the general anti-apoptotic activity of TUDCA can be leveraged against *C. difficile* toxins.

A recent preprint corroborated our findings that conjugated bile acids are protective against cytotoxic compounds (56). Unconjugated bile acids increased the permeability of Caco-2 monolayers whereas conjugated bile acids prevented this disruption of membrane integrity by forming micelles around unconjugated bile acids. To increase levels of conjugated bile acids in the intestine, rats fed a choline-deficient, high-fat diet were given the bile salt hydrolase inhibitor AAA-10. AAA-10 rats had elevated cecal TUDCA which was associated with improved barrier integrity and decreased intestinal and hepatic inflammation. A similar strategy could be applied to mouse models of CDI to assess the protective role of conjugated bile acids *in vivo*. Manipulating the bile acid pool is currently being explored as a therapeutic strategy for CDI. Our findings demonstrate that alterations to the bile acid pool, specifically deconjugation, may have detrimental effects on the host. While deconjugation is the first step to produce secondary bile acids that are inhibitory against *C. difficile* growth, an increase in unconjugated bile acids could potentially damage intestinal epithelial cell membranes or activate proapoptotic pathways, leading to exacerbated cell death and inflammation. When designing therapies that alter the bile acid pool, careful consideration is needed to avoid the production of toxic concentrations of unconjugated bile acids in the intestine.

## MATERIALS AND METHODS

**Stains, cell lines, and reagents.** *C. difficile* strains R20291 and R20291  $\Delta$ tcdR were used in this study (35). *C. difficile* spores were maintained on brain heart infusion (BHI) medium supplemented with 100 mg/L L-cysteine and 0.1% taurocholate (Sigma-Aldrich, T4009). Cultures were started by inoculating a single colony from the plate into BHI liquid medium supplemented with 100 mg/L L-cysteine and grown anaerobically. Caco-2 (ATCC, HTB-37), HCT116 (ATCC, CCL-247), IM90 (ATCC, CCL-186) and Vero cells (ATCC, CCL-81) were cultured in DMEM supplemented with 2 mM L-glutamine and 10% FBS and incubated in 5% CO<sub>2</sub> at 37°C. CellEvent Caspase-3/7 Green Detection Reagent (C10723) and PrestoBlue Cell Viability Reagent (A13261) were purchased from ThermoFisher Scientific. All bile acids were dissolved in DMSO to a final concentration of 40 mM. Vendors and catalog numbers of bile acids used in this study are listed in Table S1 in the supplemental material. Staurosporine (S6942) was purchased from MilliporeSigma. Commercially available *C. difficile* toxins (A and B) and antitoxin for the Vero cell assay were purchased from List Biological Labs (Toxin A:152C and Toxin B: 155C) and TechLabs (T5000), respectively. The plasmid pDSW1728-PtcdA::mCherry was a kind gift from Dr. Craig Ellermeier (University of Iowa). All strains, plasmids, and primers used in this study are listed in Table S2.

**Protein expression and purification.** Plasmid pHis1522 encoding his-tagged TcdB was a kind gift from Hanping Feng and plasmid pHis1522 encoding his-tagged TcdA was a kind gift from Merck. Expression and isolation of recombinant TcdB and TcdA was performed as described by Yang et al. (57). Briefly, transformed *Bacillus megaterium* was inoculated into LB containing tetracycline and grown to an A<sub>600</sub> of 1.6, followed by overnight xylose induction at 30°C. Bacterial pellets were collected, resuspended with 20 mM Tris pH 8/0.1 M NaCl, and passed twice through an EmulsiFlex C3 microfluidizer (Avestin, Ottawa, ON) at 15,000 lb/in<sup>2</sup>. The resulting lysate was clarified by centrifuging at 18,000 × g for 20 min. TcdB and TcdA were purified by nickel affinity chromatography followed by anion-exchange chromatography using HisTrap FF Crude and HiTrap Q columns (Cytiva), respectively. Fractions containing TcdB or TcdA were verified by SDS-PAGE, then pooled and diafiltered with a 100,000 MWCO ultrafiltration device (Corning) into 20 mM Tris PH 7.5/150 mM NaCl. Finally, glycerol was added to 5% vol/vol, the protein concentration was estimated by A280, divided into single use aliquots, and stored at -80°C.

**Caspase-3/7 activation assay.** Activation of Caspases 3 and 7 was assessed using CellEvent Caspase-3/7 Green Detection Reagent according to the manufacturer's instructions. Caco-2 cells or HCT116 cells were seeded in 96-well plates for 7 days or until confluent. DMEM containing recombinantly purified TcdA and TcdB (30 pmol) or filtered *C. difficile* supernatants (1:500) were added to the wells and the plates were incubated for 8 h at 37°C before the media was replaced with fresh DMEM containing bile acids. After 24 h of incubation, the media was replaced with 1X PBS containing 5% FBS and 2 μM CellEvent Caspase-3/7 Green Detection Reagent. The plates were incubated for 1 h at 37°C and green fluorescence was detected at excitation/emission wavelengths of 485/530 nm using a ThermoFisher Fluoroskan Plate Reader. PrestoBlue Cell Viability Reagent was then added to the wells and incubated for 30 min at 37°C. Red fluorescence was detected at excitation/emission wavelengths of 550/610 nm. Co-incubation experiments with TUDCA were performed by concurrently adding DMEM containing TUDCA (500 μM) and staurosporine (1 μM) to Caco-2 cells. Pre-incubation experiments with TUDCA were performed by adding DMEM containing staurosporine (1 μM) to Caco-2 cells for 8 h before the addition of TUDCA (500 μM). Caspase-3/7 activation and cell viability were measured 24 h later as described above. Data are displayed as the ratio of caspase activation RFU to cell viability RFU and normalized to the DMSO control.

**Differential scanning fluorometry.** DSF was performed in a similar manner as described previously (58). Recombinantly purified TcdB protein was diluted to 0.05 μg/μL using phosphate buffer (100 mM KPO<sub>4</sub>, 150 mM NaCl, pH 7) containing 5X SYPRO Orange (Invitrogen S6650), and a serial dilution of test compound. A Bio-Rad CFX96 qRT-PCR thermocycler was used to establish a temperature gradient from 42°C to 65°C in 0.5°C increments, while simultaneously recording the increase in SYPRO Orange fluorescence as a consequence of binding to hydrophobic regions exposed on unfolded proteins. The Bio-Rad CFX Manager 3.1 software was used to integrate the fluorescence curves to calculate the melting point.

**Arrayscan high content imaging.** IMR90 cells were grown in EMEM (Wisent) supplemented with 10% FBS and penicillin-streptomycin (complete EMEM) and were seeded in 96-well Cellbind plates (Corning) at a density of 3,000 cells/well. After 48 h, the media was exchanged with serum free EMEM (SFM) containing 1 μM Celltracker Orange CMRA (Invitrogen C34551). After 60 min, excess dye was removed by media exchange with 90 μL SFM. An Agilent Bravo liquid handler was used to deliver 0.4 μL of compound from the compound plate to the cell plate, immediately followed by 10 μL of recombinantly purified TcdB (5 pM diluted in SFM), representing a final concentration of toxin (0.5 pM) previously established as EC99 levels of cytopathology. The cell plates were returned to the incubator for 3.5 h before imaging. Celltracker-labeled cells were evaluated on a Cellomics ArrayScan VTI HCS reader (Thermo Scientific, Waltham, MA) using the Target Acquisition mode, a 10× objective and a sample rate of at least 150 objects per well. After recording all image data, the cell rounding and shrinking effects of TcdB intoxication were calculated using the cell rounding index (CRI), a multiple of the length-to-width ratio and area parameters. The percent inhibition was calculated as the ratio between the sample well and the average toxin-untreated controls after subtracting the average DMSO control values. Dose response curves were created and evaluated using Prism software (GraphPad Software, La Jolla, CaA).

**RNA extraction from Caco-2 cells.** Caco-2 cells were grown in 24-well plates for 21 days with media changes on every third day. Recombinantly purified TcdA and TcdB (30 pmol) were added to the wells for 8 h before the addition of either UDCA or TUDCA (500 μM). RNA for Nanostring analysis was extracted from Caco-2 cells 24 h later using the PureLink RNA minikit (Thermo Fisher, 12183025) following the manufacturer's protocol. The RNA was treated with Turbo DNase (Thermo Fisher, AM2239) to

remove genomic DNA contamination. RNA was then column purified according to the manufacturer's instructions (Zymo, R1019) and RNA integrity was assessed via qubit and nanodrop.

**NanoString analysis.** RNA from Caco-2 cells was submitted to the DELTA Translational Recharge Center at the University of North Carolina at Chapel Hill for quantification of transcripts via NanoString technology. The nCounter Human Host Response gene expression panel was purchased from NanoString Technologies (Seattle, WA). The raw data were normalized to six internal reference genes using nSolver software following the manufacturer's instructions (NanoString Technologies).

Log<sub>2</sub> fold changes and significance in gene expression fold change were identified using nSolver Advanced analysis software. Enriched GO biological terms and KEGG pathways were identified using ShinyGO with a FDR cut off 0.05 (59). Enriched pathways were visualized in Prism 9.

**Quantitative reverse transcription-PCR.** RNA from Caco-2 cells was used as the template in reverse transcription reactions using the High-Capacity cDNA Reverse transcription kit (ThermoFisher 4368814) following the manufacturer's protocol. The resulting cDNA was diluted 1:5 in deionized water and used as the template for quantitative PCR with the SsoAdvanced Universal SYBR green Supermix (Bio-Rad). For relative quantification, the  $\Delta\Delta C_t$  method was used to normalize *CCR1*, *CCL15*, *CCL16* and *MYC* genes to that of the internal control, *GAPDH*.

**Lysotracker assay.** Endosomal pH neutralization was assayed as described by Slater et al. (60); IMR90 cells in complete EMEM were plated at 14,000 cells/well (~95% confluence). After 24 h the media was changed to serum free media for 60 min, then bile acid was added and incubated at 37°C for 2 h. Lysotracker red DND-99 (Life Technologies) was added to 0.1  $\mu$ M, and incubated for 30 min. Excess dye was removed by media change and the fluorescence at ex/em 574/594 was measured on a Biotek Neo plate reader (Agilent Technologies).

**Spore preparation.** Spores were prepared as in Edwards and McBride (61). Mid-log phase cultures were spread onto 70:30 agar plates and incubated at 37°C for 4 days. The bacterial lawns were scraped off and suspended in 10 mL sterile PBS, mixed 1:1 with 96% ethanol, vortexed for 30 sec, and incubated at room temperature for 1 h. The suspension was centrifuged at 3,000 rpm for 10 min. The pellet was suspended in 10 mL fresh sterile PBS and centrifuged again; this was repeated twice. The final pellet was suspended in 1 mL PBS and serial dilutions were plated on BHI agar with 0.1% of taurocholate for spore CFU enumeration.

***C. difficile* in vitro spore germination assay.** This assay was performed as previously described (62). Purified spores were enumerated and tested for purity before use and were subjected to heat treatment (65°C for 20 min) to eliminate any vegetative cells. UDCA and TUDCA were dissolved in DMSO, passed into the anaerobic chamber, and added to BHI broth containing 0.1% TCA. CDCA (0.04%), a known inhibitor of TCA-mediated spore germination, was used as a negative control. The spore stock was resuspended in BHI broth containing bile acids to an OD<sub>600</sub> of 0.3. The OD<sub>600</sub> was measured at 0, 20, 40, and 60 min using a Tecan Infinite F200 Pro plate reader. Data are plotted as ratios of the OD<sub>600</sub> at the indicated time points to the OD<sub>600</sub> at time zero against time.

***C. difficile* growth assay.** *C. difficile* R20291 was started from a single colony and grown anaerobically in 5 mL of BHI overnight, subcultured 1:5 in BHI, and grown to mid-log phase (OD, 0.3 to 0.5). Cultures were then diluted to an OD of 0.01 in fresh BHI medium supplemented with either DMSO, UDCA or TUDCA (500  $\mu$ M) and incubated for 24 h. At 0 and 24 h time points, culture aliquots were enumerated on BHI plates to obtain total CFU per milliliter.

***C. difficile* in vitro Vero cell cytotoxicity assay.** Culture supernatants from the anaerobic growth assay were filtered through a 0.22 micron filter and 10-fold dilutions, to a maximum of 10<sup>-6</sup>, were generated. Sample dilutions were incubated 1:1 with 1X PBS (for all dilutions) or antitoxin (performed for 10<sup>-1</sup> and 10<sup>-4</sup> dilutions only) for 40 min at room temperature. Following incubation, these mixtures were added to the Vero cells seeded in 96-well plates, and the plates were incubated overnight at 37°C. Vero cells were viewed under 200 $\times$  magnification for rounding after overnight incubation. The cytotoxic titer was defined as the reciprocal of the highest dilution that produced rounding in 80% of Vero cells for each sample. Vero cells treated with commercially available *C. difficile* TcdA and TcdB (List Biological Labs, 152C and 155C) and antitoxin were used as controls.

**mCherry fluorescence reporter assay.** R20291 strains carrying either pDSW1728-*PtcdA::mCherry* or pDSW1728 were grown anaerobically on BHI agar + 10  $\mu$ g/mL thiamphenicol. A single colony was inoculated into a 5 mL culture of BHI broth + 10  $\mu$ g/mL thiamphenicol and grown overnight at 37°C. The overnight culture was diluted 1:100 into a fresh 3 mL culture of BHI broth + 3  $\mu$ g/mL thiamphenicol + either DMSO UDCA or TUDCA (500  $\mu$ M) and grown at 37°C. After 24 h of growth, a 500- $\mu$ L aliquot of culture was mixed with 120  $\mu$ L of a 5X fixation cocktail: 100  $\mu$ L of 16% paraformaldehyde aqueous solution and 20  $\mu$ L of 1 M NaPO<sub>4</sub> buffer (pH 7.4). The sample was incubated at room temperature for 30 min, removed from the anaerobic chamber and incubated in the dark for 30 min on ice. The fixed cells were washed three times with 1X PBS, resuspended in 30  $\mu$ L of PBS and left in the dark at 4°C overnight to allow for chromophore maturation. Red fluorescence was measured at excitation/emission wavelengths of 550/610 nm using a Tecan Infinite F200 Pro plate reader. Absorbance at 600 nm was measured on the same plate reader. Data are displayed as the ratio of fluorescence to absorbance.

**Statistical analysis.** All statistical tests were performed in GraphPad Prism 9 (GraphPad, CA, USA). Statistical significance was set at a *P* value of <0.05 for all analyses. A Student's *t* test with Welch's correction was used when comparing two groups. A two-way ANOVA with Sidak's correction for multiple comparisons was used when comparing multiple groups. nSolver Advanced Analysis software was to calculate significance in gene expression fold changes.

## SUPPLEMENTAL MATERIAL

Supplemental material is available online only.

**SUPPLEMENTAL FILE 1**, PDF file, 1.1 MB.

**SUPPLEMENTAL FILE 2**, XLSX file, 0.04 MB.

**SUPPLEMENTAL FILE 3**, XLSX file, 0.01 MB.

**SUPPLEMENTAL FILE 4**, XLSX file, 0.04 MB.

**SUPPLEMENTAL FILE 5**, XLSX file, 0.01 MB.

**SUPPLEMENTAL FILE 6**, XLSX file, 0.1 MB.

## ACKNOWLEDGMENTS

C.M.P. and C.M.T. are funded by the National Institute of General Medical Sciences of the National Institutes of Health under award number R35GM119438. This project was also funded by an intramural grant from the North Carolina State University College of Veterinary Medicine.

C.M.T. consults for Vedanta Biosciences, Inc., Summit Therapeutics. C.M.T. is a founder of CRISPR Biotechnologies.

## REFERENCES

- Guh AY, Mu Y, Winston LG, Johnston H, Olson D, Farley MM, Wilson LE, Holzbauer SM, Phipps EC, Dumyati GK, Beldavs ZG, Kainer MA, Karlsson M, Gerding DN, McDonald LC, Emerging Infections Program Clostridioides Difficile Infection Working Group. 2020. Trends in U.S. burden of Clostridioides difficile infection and outcomes. *N Engl J Med* 382:1320–1330. <https://doi.org/10.1056/NEJMoa1910215>.
- Aktories K, Schwan C, Jank T. 2017. Clostridium difficile toxin biology. *Annu Rev Microbiol* 71:281–307. <https://doi.org/10.1146/annurev-micro-090816-093458>.
- Smits WK, Lyras D, Lacy DB, Wilcox MH, Kuijper EJ. 2016. *Clostridium difficile* infection. *Nat Rev Dis Primers* 2:16020. <https://doi.org/10.1038/nrdp.2016.20>.
- McDonald LC, Gerding DN, Johnson S, Bakken JS, Carroll KC, Coffin SE, Dubberke ER, Garey KW, Gould CV, Kelly C, Loo V, Shaklee Sammons J, Sandora TJ, Wilcox MH. 2018. Clinical practice guidelines for Clostridium difficile infection in adults and children: 2017 update by the Infectious Diseases Society of America (IDSA) and Society for Healthcare Epidemiology of America (SHEA). *Clin Infect Dis* 66:e1–e48. <https://doi.org/10.1093/cid/cix1085>.
- Wolf J, Kalocsai K, Fortuny C, Lazar S, Bosis S, Korczowski B, Petit A, Bradford D, Croos-Dabrera R, Incera E, Melis J. 2020. Safety and efficacy of fidaxomicin and vancomycin in children and adolescents with Clostridioides (Clostridium) difficile infection: a phase 3, multicenter, randomized, single-blind clinical trial (SUNSHINE). *Clin Infect Dis* 71:2581–2588.
- Beinortas T, Burr NE, Wilcox MH, Subramanian V. 2018. Comparative efficacy of treatments for Clostridium difficile infection: a systematic review and network meta-analysis. *Lancet Infect Dis* 18:1035–1044. [https://doi.org/10.1016/S1473-3099\(18\)30285-8](https://doi.org/10.1016/S1473-3099(18)30285-8).
- Slimings C, Riley TV. 2014. Antibiotics and hospital-acquired Clostridium difficile infection: update of systematic review and meta-analysis. *J Antimicrob Chemother* 69:881–891. <https://doi.org/10.1093/jac/dkt477>.
- Solomon K, Martin AJ, O'Donoghue C, Chen X, Fenelon L, Fanning S, Kelly CP, Kyne L. 2013. Mortality in patients with Clostridium difficile infection correlates with host pro-inflammatory and humoral immune responses. *J Med Microbiol* 62:1453–1460. <https://doi.org/10.1099/jmm.0.058479-0>.
- El Feghaly RE, Stauber JL, Deych E, Gonzalez C, Tarr PI, Haslam DB. 2013. Markers of intestinal inflammation, not bacterial burden, correlate with clinical outcomes in Clostridium difficile infection. *Clin Infect Dis* 56:1713–1721. <https://doi.org/10.1093/cid/cit147>.
- Yu H, Chen K, Sun Y, Carter M, Garey KW, Savidge TC, Devaraj S, Tessier ME, von Rosenvinge EC, Kelly CP, Pasetti MF, Feng H. 2017. Cytokines are markers of the Clostridium difficile-induced inflammatory response and predict disease severity. *Clin Vaccine Immunol* 24. <https://doi.org/10.1128/CVI.00037-17>.
- Dieterle MG, Putler R, Perry DA, Menon A, Abernathy-Close L, Perlman NS, Penkevich A, Standke A, Keidan M, Vendrov KC, Bergin IL, Young VB, Rao K. 2020. Systemic inflammatory mediators are effective biomarkers for predicting adverse outcomes in Clostridioides difficile infection. *mBio* 11. <https://doi.org/10.1128/mBio.00180-20>.
- Hofmann AF, Mysels KJ. 1992. Bile acid solubility and precipitation in vitro and in vivo: the role of conjugation, pH, and Ca<sup>2+</sup> ions. *J Lipid Res* 33:617–626. [https://doi.org/10.1016/S0022-2275\(20\)41426-9](https://doi.org/10.1016/S0022-2275(20)41426-9).
- Hofmann AF, Hagey LR. 2008. Bile acids: chemistry, pathochemistry, biology, pathobiology, and therapeutics. *Cell Mol Life Sci* 65:2461–2483. <https://doi.org/10.1007/s00018-008-7568-6>.
- Winston JA, Theriot CM. 2020. Diversification of host bile acids by members of the gut microbiota. *Gut Microbes* 11:158–171. <https://doi.org/10.1080/19490976.2019.1674124>.
- Foley MH, O'Flaherty S, Barrangou R, Theriot CM. 2019. Bile salt hydrolases: Gatekeepers of bile acid metabolism and host-microbiome cross-talk in the gastrointestinal tract. *PLoS Pathog* 15:e1007581. <https://doi.org/10.1371/journal.ppat.1007581>.
- Quinn RA, Melnik AV, Vrbanac A, Fu T, Patras KA, Christy MP, Bodai Z, Belda-Ferre P, Tripathi A, Chung LK, Downes M, Welch RD, Quinn M, Humphrey G, Panitchpakdi M, Weldon KC, Aksenov A, da Silva R, Avila-Pacheco J, Clish C, Bae S, Mallick H, Franzosa EA, Lloyd-Price J, Bussell R, Thron T, Nelson AT, Wang M, Leszczynski E, Vargas F, Gauglitz JM, Meehan MJ, Gentry E, Arthur TD, Komor AC, Poulsen O, Boland BS, Chang JT, Sandborn WJ, Lim M, Garg N, Lumeng JC, Xavier RJ, Kazmierczak BI, Jain R, Egan M, Rhee KE, Ferguson D, Raffatellu M, Vlamakis H, et al. 2020. Global chemical effects of the microbiome include new bile-acid conjugations. *Nature* 579:123–129. <https://doi.org/10.1038/s41586-020-2047-9>.
- Theriot CM, Koenigsnecht MJ, Carlson PE, Hatton GE, Nelson AM, Li B, Huffnagle GB, Z Li J, Young VB. 2014. Antibiotic-induced shifts in the mouse gut microbiome and metabolome increase susceptibility to Clostridium difficile infection. *Nat Commun* 5:3114. <https://doi.org/10.1038/ncomms4114>.
- Theriot CM, Bowman AA, Young VB. 2016. Antibiotic-induced alterations of the gut microbiota alter secondary bile acid production and allow for Clostridium difficile spore germination and outgrowth in the large intestine. *mSphere* 1. <https://doi.org/10.1128/mSphere.00045-15>.
- Koenigsnecht MJ, Theriot CM, Bergin IL, Schumacher CA, Schloss PD, Young VB. 2015. Dynamics and establishment of Clostridium difficile infection in the murine gastrointestinal tract. *Infect Immun* 83:934–941. <https://doi.org/10.1128/IAI.02768-14>.
- Thanissery R, Winston JA, Theriot CM. 2017. Inhibition of spore germination, growth, and toxin activity of clinically relevant C. difficile strains by gut microbiota derived secondary bile acids. *Anaerobe* 45:86–100. <https://doi.org/10.1016/j.anaerobe.2017.03.004>.
- Sorg JA, Sonenshein AL. 2008. Bile salts and glycine as Cogerminants for Clostridium difficile spores. *J Bacteriol* 190:2505–2512. <https://doi.org/10.1128/JB.01765-07>.
- Tam J, Icho S, Utama E, Orrell KE, Gómez-Biagi RF, Theriot CM, Kroh HK, Rutherford SA, Lacy DB, Melnyk RA. 2020. Intestinal bile acids directly modulate the structure and function of C. difficile TcdB toxin. *Proc Natl Acad Sci U S A* 117:6792–6800. <https://doi.org/10.1073/pnas.1916965117>.
- Winston JA, Rivera AJ, Cai J, Thanissery R, Montgomery SA, Patterson AD, Theriot CM. 2020. Ursodeoxycholic acid (UDCA) mitigates the host inflammatory response during Clostridioides difficile infection by altering gut bile acids. *Infect Immun* 88. <https://doi.org/10.1128/IAI.00045-20>.

24. Cai J, Sun L, Gonzalez FJ. 2022. Gut microbiota-derived bile acids in intestinal immunity, inflammation, and tumorigenesis. *Cell Host Microbe* 30:289–300. <https://doi.org/10.1016/j.chom.2022.02.004>.
25. Amaral JD, Viana RJ, Ramalho RM, Steer CJ, Rodrigues CM. 2009. Bile acids: regulation of apoptosis by ursodeoxycholic acid. *J Lipid Res* 50:1721–1734. <https://doi.org/10.1194/jlr.R900011-JLR200>.
26. Donkers JM, Roscam Abbing RLP, van de Graaf SFJ. 2019. Developments in bile salt based therapies: a critical overview. *Biochem Pharmacol* 161:1–13. <https://doi.org/10.1016/j.bcp.2018.12.018>.
27. Fiorucci S, Biagioli M, Zampella A, Distrutti E. 2018. Bile acids activated receptors regulate innate immunity. *Front Immunol* 9:1853. <https://doi.org/10.3389/fimmu.2018.01853>.
28. Flegel WA, Muller F, Daubener W, Fischer HG, Hadding U, Northoff H. 1991. Cytokine response by human monocytes to *Clostridium difficile* toxin A and toxin B. *Infect Immun* 59:3659–3666. <https://doi.org/10.1128/iai.59.10.3659-3666.1991>.
29. Sun H, Chow EC, Liu S, Du Y, Pang KS. 2008. The Caco-2 cell monolayer: usefulness and limitations. *Expert Opin Drug Metab Toxicol* 4:395–411. <https://doi.org/10.1517/17425255.4.4.395>.
30. Powell AA, LaRue JM, Batta AK, Martinez JD. 2001. Bile acid hydrophobicity is correlated with induction of apoptosis and/or growth arrest in HCT116 cells. *Biochem J* 356:481–486. <https://doi.org/10.1042/bj3560481>.
31. Qa'Dan M, Spyres LM, Ballard JD. 2000. pH-induced conformational changes in *Clostridium difficile* toxin B. *Infect Immun* 68:2470–2474. <https://doi.org/10.1128/IAI.68.5.2470-2474.2000>.
32. Tam J, Beilhartz GL, Auger A, Gupta P, Therien AG, Melnyk RA. 2015. Small molecule inhibitors of *Clostridium difficile* toxin B-induced cellular damage. *Chem Biol* 22:175–185. <https://doi.org/10.1016/j.chembiol.2014.12.010>.
33. Rodemann JF, Dubberke ER, Reske KA, Seo DH, Stone CD. 2007. Incidence of *Clostridium difficile* infection in inflammatory bowel disease. *Clinical gastroenterology and hepatology: the official clinical practice journal of the Clin Gastroenterol Hepatol* 5:339–344. <https://doi.org/10.1016/j.cgh.2006.12.027>.
34. Binion DG. 2012. *Clostridium difficile* infection in patients with inflammatory bowel disease. *Gastroenterol Hepatol* 8:615–617.
35. Fletcher JR, Pike CM, Parsons RJ, Rivera AJ, Foley MH, McLaren MR, Montgomery SA, Theriot CM. 2020. *Clostridioides difficile* exploits toxin-mediated inflammation to alter the host nutritional landscape and exclude competitors from the gut microbiota. *bioRxiv*.
36. Jarchum I, Liu M, Shi C, Equinda M, Pamer EG. 2012. Critical role for MyD88-mediated neutrophil recruitment during *Clostridium difficile* colitis. *Infect Immun* 80:2989–2996. <https://doi.org/10.1128/IAI.00448-12>.
37. Abt MC, Lewis BB, Caballero S, Xiong H, Carter RA, Sušac B, Ling L, Leiner I, Pamer EG. 2015. Innate immune defenses mediated by two ILC subsets are critical for protection against acute *Clostridium difficile* infection. *Cell Host Microbe* 18:27–37. <https://doi.org/10.1016/j.chom.2015.06.011>.
38. Saleh MM, Frisbee AL, Leslie JL, Buonomo EL, Cowardin CA, Ma JZ, Simpson ME, Scully KW, Abhyankar MM, Petri WA. 2019. Colitis-induced Th17 cells increase the risk for severe subsequent *Clostridium difficile* infection. *Cell Host Microbe* 25:756–765 e5. <https://doi.org/10.1016/j.chom.2019.03.003>.
39. Abhyankar MM, Ma JZ, Scully KW, Nafziger AJ, Frisbee AL, Saleh MM, Madden GR, Hays AR, Poulter M, Petri WA. 2020. Immune profiling to predict outcome of *Clostridioides difficile* infection. *mBio* 11. <https://doi.org/10.1128/mBio.00905-20>.
40. Attili AF, Angelico M, Cantafora A, Alvaro D, Capocaccia L. 1986. Bile acid-induced liver toxicity: relation to the hydrophobic-hydrophilic balance of bile acids. *Med Hypotheses* 19:57–69. [https://doi.org/10.1016/0306-9877\(86\)90137-4](https://doi.org/10.1016/0306-9877(86)90137-4).
41. Barrasa JI, Olmo N, Lizarbe MA, Turnay J. 2013. Bile acids in the colon, from healthy to cytotoxic molecules. *Toxicol in Vitro* 27:964–977. <https://doi.org/10.1016/j.tiv.2012.12.020>.
42. Saavedra PHV, Huang L, Ghazavi F, Kourula S, Vanden Berghe T, Takahashi N, Vandenabeele P, Lamkanfi M. 2018. Apoptosis of intestinal epithelial cells restricts *Clostridium difficile* infection in a model of pseudomembranous colitis. *Nat Commun* 9:4846. <https://doi.org/10.1038/s41467-018-07386-5>.
43. Matarrese P, Falzano L, Fabbri A, Gambardella L, Frank C, Geny B, Popoff MR, Malorni W, Fiorentini C. 2007. *Clostridium difficile* toxin B causes apoptosis in epithelial cells by thrilling mitochondria. Involvement of ATP-sensitive mitochondrial potassium channels. *J Biol Chem* 282:9029–9041. <https://doi.org/10.1074/jbc.M607614200>.
44. Brandes V, Schelle I, Brinkmann S, Schulz F, Schwarz J, Gerhard R, Genth H. 2012. Protection from *Clostridium difficile* toxin B-catalysed Rac1/Cdc42 glycosylation by tauroursodeoxycholic acid-induced Rac1/Cdc42 phosphorylation. *Biol Chem* 393:77–84. <https://doi.org/10.1515/BC-2011-198>.
45. Lee YY, Hong SH, Lee YJ, Chung SS, Jung HS, Park SG, Park KS. 2010. Tauroursodeoxycholate (TUDCA), chemical chaperone, enhances function of islets by reducing ER stress. *Biochem Biophys Res Commun* 397:735–739. <https://doi.org/10.1016/j.bbrc.2010.06.022>.
46. Zlotnik A, Yoshie O. 2012. The chemokine superfamily revisited. *Immunity* 36:705–716. <https://doi.org/10.1016/j.immuni.2012.05.008>.
47. Morteau O, Castagliuolo I, Mykoniatis A, Zacks J, Wilk M, Lu B, Akis CP, Gerard NP, Gerard C. 2002. Genetic deficiency in the chemokine receptor CCR1 protects against acute *Clostridium difficile* toxin A enteritis in mice. *Gastroenterology* 122:725–733. <https://doi.org/10.1053/gast.2002.31873>.
48. Zhang Z, Zheng M, Bindas J, Schwarzenberger P, Kolls JK. 2006. Critical role of IL-17 receptor signaling in acute TNBS-induced colitis. *Inflamm Bowel Dis* 12:382–388. <https://doi.org/10.1097/01.MIB.0000218764.06959.91>.
49. Ogawa A, Andoh A, Araki Y, Bamba T, Fujiyama Y. 2004. Neutralization of interleukin-17 aggravates dextran sulfate sodium-induced colitis in mice. *Clin Immunol* 110:55–62. <https://doi.org/10.1016/j.clim.2003.09.013>.
50. Cuevas E, Burks S, Raymick J, Robinson B, Gomez-Crisostomo NP, Escudero-Lourdes C, Lopez AG, Chigurupati S, Hanig J, Ferguson SA, Sarkar S. 2020. Tauroursodeoxycholic acid (TUDCA) is neuroprotective in a chronic mouse model of Parkinson's disease. *Nutr Neurosci*:1–18.
51. Zhou L, Liu Z, Chen S, Qiu J, Li Q, Wang S, Zhou W, Chen D, Yang G, Guo L. 2021. Transcription factor EB-mediated autophagy promotes dermal fibroblast differentiation and collagen production by regulating endoplasmic reticulum stress and autophagy-dependent secretion. *Int J Mol Med* 47:547–560. <https://doi.org/10.3892/ijmm.2020.4814>.
52. Van den Bossche L, Hindryckx P, Devisscher L, Devriese S, Van Welden S, Holvoet T, Vilchez-Vargas R, Vital M, Pieper DH, Vanden Bussche J, Vanhaecke L, Van de Wiele T, De Vos M, Laukens D. 2017. Ursodeoxycholic acid and its taurine- or glycine-conjugated species reduce colitogenic dysbiosis and equally suppress experimental colitis in mice. *Appl Environ Microbiol* 83. <https://doi.org/10.1128/AEM.02766-16>.
53. Laukens D, Devisscher L, Van den Bossche L, Hindryckx P, Vandenbroucke RE, Vandewynckel Y-P, Cuvellier C, Brinkman BM, Libert C, Vandenabeele P, De Vos M. 2014. Tauroursodeoxycholic acid inhibits experimental colitis by preventing early intestinal epithelial cell death. *Lab Invest* 94:1419–1430. <https://doi.org/10.1038/labinvest.2014.117>.
54. Cao SS, Zimmermann EM, Chuang B-M, Song B, Nwokoye A, Wilkinson JE, Eaton KA, Kaufman RJ. 2013. The unfolded protein response and chemical chaperones reduce protein misfolding and colitis in mice. *Gastroenterology* 144:989–1000.e6. <https://doi.org/10.1053/j.gastro.2013.01.023>.
55. Van den Bossche L, Borsboom D, Devriese S, Van Welden S, Holvoet T, Devisscher L, Hindryckx P, De Vos M, Laukens D. 2017. Tauroursodeoxycholic acid protects bile acid homeostasis under inflammatory conditions and dampens Crohn's disease-like ileitis. *Lab Invest* 97:519–529. <https://doi.org/10.1038/labinvest.2017.6>.
56. Li DK, Chaudhari SN, Sojoodi M, Lee Y, Adhikari AA, Zuckerberg L, Shroff S, Barrett SC, Tanabe K, Chung RT, Devlin AS. 2021. Inhibition of microbial deconjugation of micellar bile acids protects against intestinal permeability and liver injury. *bioRxiv*.
57. Yang G, Zhou B, Wang J, He X, Sun X, Nie W, Tzipori S, Feng H. 2008. Expression of recombinant *Clostridium difficile* toxin A and B in *Bacillus megaterium*. *BMC Microbiol* 8:192. <https://doi.org/10.1186/1471-2180-8-192>.
58. Niesen FH, Berglund H, Vedadi M. 2007. The use of differential scanning fluorimetry to detect ligand interactions that promote protein stability. *Nat Protoc* 2:2212–2221. <https://doi.org/10.1038/nprot.2007.321>.
59. Ge SX, Jung D, Yao R. 2020. ShinyGO: a graphical gene-set enrichment tool for animals and plants. *Bioinformatics* 36:2628–2629. <https://doi.org/10.1093/bioinformatics/btz931>.
60. Slater LH, Hett EC, Mark K, Chumbler NM, Patel D, Lacy DB, Collier RJ, Hung DT. 2013. Identification of novel host-targeted compounds that protect from anthrax lethal toxin-induced cell death. *ACS Chem Biol* 8:812–822. <https://doi.org/10.1021/cb300555n>.
61. Edwards AN, McBride SM. 2016. Isolating and purifying *Clostridium difficile* spores. *Methods Mol Biol* 1476:117–128. [https://doi.org/10.1007/978-1-4939-6361-4\\_9](https://doi.org/10.1007/978-1-4939-6361-4_9).
62. Sorg JA, Sonenshein AL. 2010. Inhibiting the initiation of *Clostridium difficile* spore germination using analogs of chenodeoxycholic acid, a bile acid. *J Bacteriol* 192:4983–4990. <https://doi.org/10.1128/JB.00610-10>.